Embedded Pipes: Static Investigation of Embedded Conduits with Consideration Given to Their Elasticity
Voellmy, A.

Publisher's version / Version de l'éditeur:
https://doi.org/10.4224/20386606
Translation (National Research Council of Canada), 1949-11-01

NATIONAL RESEARCH COUNCIL OF CANADA

Technical Translation TT-131

Title: Embedded pipes.

(Eingebettete Rohre).

Author: Adolf Voellmy.

Reference: Proc. Inst. Building Statics, Zurich, 1937.

Translator: H.L. Kasten.

F O R E W O R D

The following pages contain a translation of Voellmy's paper on Eingebettete Rohre (Embedded Pipes). This paper was published in 1937 by Gebs. Leeman & Co., Zurich and Leipzig, as a proceeding of the Institute of Building Statics, Federal Institute of Technology, Zurich.

The paper consists of four main sections as follows:

(a) Earth pressures on embedded structures without consideration of deformation conditions.

(b) The stressing of embedded structures dependent on their deformations.

(c) Research.

(d) The practical computation of embedded pipes.

The whole field of stresses due to earth pressure on buried structures is quite complicated and few engineers have the basic mathematical knowledge, or the time, to go into detailed theoretical studies of the subject. However, the practical application of Voellmy's analysis is not difficult and, due to the outstanding importance of the topic, it seemed to the writer that a translation of the fourth chapter would be well worth while in order to make available to other engineers what seems to him an excellent method of design of underground conduits.

In spite of a very busy academic session, Mr. Kasten has very kindly devoted much of his leisure time to writing out the translation. The figures have been reproduced by photography and the German words substituted by their English equivalents.

It is hoped that this monograph will be found to be immediately useful in the design of such structures as properly come within its scope.

I.F. Morrison.

PREFACE

The National Research Council, through its Division of Building Research, is pleased to have been able to arrange for the publication of this translation of an important paper in the field of civil engineering. The significance of the paper is indicated in the Foreword by Professor I. F. Morrison, of the University of Alberta, who brought the translation to the attention of the undersigned.

The publication of this translation represents one way in which the Division of Building Research hopes to work with the engineering and architectural departments of Canadian universities in the co-operative development of building research in Canada.

November 8th, 1949

R. F. Legget,
Director.

CONTENTS OF CHAPTER IV

CHAPTER IV: THE PRACTICAL ANALYSIS OF EMBEDDED PIPES

CHAPTER IV

THE PRACTICAL ANALYSIS OF EMBEDDED PIPES

Summary

The previous chapters of this work have shown the varied earth loads possible on embedded structures, depending on the shape and deformation conditions of the structure. Great numbers of individual investigations concerning the most important problems in soil mechanics would be necessary to gain the complete picture of the stressing of embedded works, whereafter the necessarily simplified assumptions for their practical analysis could properly be adopted. The principles of static analysis developed in the previous chapters are applicable to embedded structures of several different forms. Since in many cases a circular cross-section allows a "closed" mathematical analysis, this investigation has dealt mainly with pipes. Furthermore, the investigation is narrowed down by considering only pipes embedded at a constant depth along their axes.

In this chapter the computations for the pressures on embedded pipes are brought together in simplified form. For sake of completeness, the computation for stresses in pipes due to surface loads, dead weight, and inner and outer water pressure have also been included.

In conclusion a few figures on the strengths and moduli of elasticity of various pipe materials have been given, as well as on factors of safety.

1. STRESSES WITH THE PIPE ON LINEAR SUPPORT

The computation of inner stresses of the pipe which follows immediately is based on the assumption that the pipe rests on a linear support. Later, in section 2 of this chapter, the added effect of a distributed reaction pressure is investigated. As the usual methods of analysing stresses in pipes under given external loads offers nothing fundamentally new, a repetition herein of the rather complicated developments and formulae was avoided, and only the internal forces at the crown, side, and sole of the pipe are given. Should the complete distribution of the internal stresses be desired for some special pipe analysis, then this may be solved in a simple manner in that a knowledge of the values of M and N at the pipe crown as given in the previous chapter makes the side-half of the pipe statically determinate. The variation of internal forces from crown to sole may be computed with no further information necessary, since those values of the internal forces at the pipe side and sole as given in the next sections serve as controls for the computation. Under all cases of symmetrical loading the shearing force at the crown disappears: $Q = 0$. It may be pointed out here that the moment on the pipe side is the maximum of the positive moments only in case the bedding of the pipe is very wide ($\alpha_0 \approx 90°$), as will be shown in the developments that follow. Normally the maximum value of the positive moment lies below the pipe side, and is up to 10% greater than the side-moment for normal earth loads.

A. EARTH PRESSURE WITHOUT REGARD TO DEFORMATION CONDITIONS

(a) Pipes in Extensive Fills.

The active earth pressure on a structure is but little affected by the deformation of the same, if the earth cover is shallow, i.e., when the depth of cover does not exceed the breadth of the structure. In this case, the earth pressure can be found using already well known earth pressure theories. Those computation methods which are based on Coulomb's theory results in good agreement with test results. In contrast, Rankine's somewhat more inaccurate application of the theory of an unbounded earth body yields a clearer picture of the pressure conditions, and was for this reason applied in this analysis. An extension of Rankine's theory was however necessary, in order to take care of all possible inclindations of the walls of embedded structures sufficiently accurately (Section I, 1 - Equation 8). As the side pressures on the embedded pipes reduce the stressing of the pipe somewhat, the usual computation is based on the lower limit of the side pressure. The distribution of the active earth pressure may then be calculated from equations (11) and (12) of Chapter 1. (See Fig. 1.)

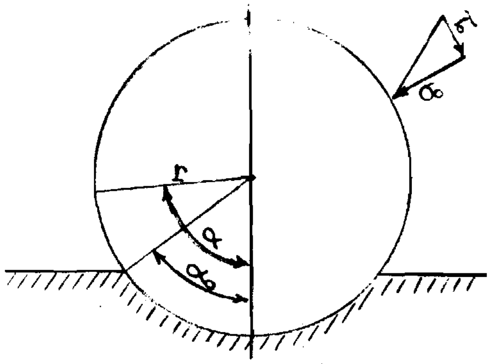

Figure 0

For the upper half of the pipe:

$$\sigma_o = \frac{\gamma}{1 + \sin\rho}(t_o + r \cdot \cos\alpha)\ (1 + \sin\rho \cdot \cos 2\alpha)^{*} \qquad (1)$$

$$\tau_o = \frac{\gamma}{1 + \sin\rho}(t_o + r \cdot \cos\alpha)\ (\sin\rho \cdot \sin 2\alpha)$$

For the lower half of the pipe:

$$\sigma_u = \sigma_o\left(1 - \frac{\tan\rho}{\tan\alpha}\right)^2 \qquad (2)$$

$$\tau_u \approx 0$$

where γ = Unit weight of fill material.

ρ = Angle of internal friction of fill material, approx. equal to its angle of repose.

t_o = Depth of fill over pipe centerline.

r = Radius of pipe (outer).

α = Angle to locate the element of the pipe wall.

The pressure distribution thus found serves as a basis for the analysis with consideration given to the rigidity of the pipe, which becomes important when depth of cover is great.

The internal stresses in the pipe due to the above given equations of pressure distribution (1 and 2) were computed based on the previously given method of pipe analysis

---

* For notation refer to Fig.0 on page 3 and to Fig. 1.

(Section II - 4 - 8 - d) and the resulting moments and normal stresses at the crown, sides, and sole of the pipe are given in Fig. 1 for various values of the angle of internal friction, ρ. The coefficients for the internal stresses (Moment, M and Normal Stress, N), assuming a linear reaction, are plotted positive outwards in a radial direction from the pipe centreline in the Figure. With these values known, the computation of the complete variation of stress throughout the pipe wall, if desired, is a simple matter, since the system is statically determinate; in this way, it is also easy to check the correctness of the given figures.

The angle of internal friction ρ may be set equal to the natural angle of repose with sufficient accuracy. Its value is not affected much by a varying moisture content of the fill material; however, the apparent cohesion (Section I - 1) increases with decreasing moisture content. For the computation of earth pressure on a pipe under fill, the effect of the cohesion may, as a rule, be allowed for in approximate fashion by increasing the angle of friction. Clayey materials back-filled in the dry state become crumbly due to the apparent cohesion, and the angle of friction for gravelly material is reached. If clayey material is put in very wet, then following drying-out, a very large reduction in side pressure takes place, again due to apparent cohesion and shrinkage. In this case, for the sake of safety, a value of the angle of internal friction $\rho \approx 90^\circ$ should be used.

The unit weight γ of loose fill material at first decreases with increasing moisture content, and reaches a minimum at a definite water content (around 3% for coarse sand). This minimum is about 15% less than the unit weight in a dry condition. On further increase in moisture content, the unit weight begins to increase and finally surpasses the weight for the dry condition. If all the voids are filled with water, then the unit weight is:

$$\gamma_n = (1 - \eta)\gamma_s + \eta\gamma_w, \text{ where}$$

γ_s = specific weight of fill material = 2.6 to 2.7 t/m^3

γ_w = specific weight of water = 1 t/m^3

$\eta = \dfrac{\gamma_s - \gamma_t}{\gamma_s}$ = porosity

γ_t = unit weight of fill material in dry condition.

If no test values for angle of internal friction and unit we ght are available, then for rough computations the following values may be used:

For gravel and sands at natural moisture content to wet, clayey materials:

Angle friction: $\rho = 35°$ to $\rho = 20°$

Unit weight: $\gamma = 1.7\ t/m^3$ to $\gamma = 2.1\ t/m^3$

(b) Pipes in Trenches

As shown previously (Section I - 6), for the case of pipes in trenches, most commonly-used backfill materials may be regarded as incompressible; in this event, the pressure on the crown of a pipe embedded in a trench with vertical or slightly outward sloping sides is found as follows:

$$q = q_o \cdot \Phi \tag{3}$$

where $q_o = \gamma . t$ = hydrostatic earth pressure

$$\Phi = \frac{1 - e^{-x}}{x} \tag{4}$$

$e = 2.718$ = base of natural logs

t = depth of cover over crown

$$x = \frac{t}{b} \cdot \tan \rho' \cdot \frac{1 - \sin \rho}{1 + \sin \rho} = \frac{t}{b} \Psi \tag{5}$$

b = half-width of trench at the level of the crown of the pipe

ρ = angle of internal friction of backfill $\approx$ natural angle of repose.

ρ' = angle of friction developed at wall of trench.

Numerical values of the function Φ may be taken from Fig. 2 for different values of the quantity $x = \frac{t}{b} \Psi$. In this Figure also, values for Ψ are given for various values of ρ, computed on the assumption that $\rho' = \rho$, which is close enough for practical purposes.

For the computation of the inner stresses in the pipe the side pressure may be neglected in most cases. This is because the backfill will likely not be properly tamped into the narrow space between pipe and trench wall; also, as shown in Section I - 5, the lateral pressure is greatly reduced in such a narrow space due to the friction with the walls.

The theoretical investigation of the same section (I - 5) also showed that it is sufficiently accurate when considering such pipes in trenches, to take the loading as evenly distributed over the horizontal projection of the pipe.

The internal stresses may then be found using the equations and coefficients of Fig. 1, if the following substitutions are made therein:

Depth of cover $t_o = t \cdot \Phi$, where Φ is taken from Fig. 2 using values of ρ, ρ' of the backfill material and trench dimensions b and t. (Reduction of vertical pressure).

Coefficients $\bar{m}$, $\bar{n} = 0$ in the equations of Fig. 1 for M and N (Vertical pressure taken as uniform over the horizontal projection).

Find values of coefficients m and n when $\rho = 90°$ from the curves of Fig. 1 and substitute these into the equations for M and N (no lateral pressure).

When these substitutions are made one arrives at the practical formulae for computation as given in Figure 2.

B. EARTH PRESSURE ON RIGID PIPES

The loading of rigid pipes forms the basis for the later investigation of the stressing of elastic pipes. Furthermore, pipes of relatively small diameter made of such materials as plain or reinforced concrete, stone blocks, or vitrified clay may be considered as completely rigid.

(a) Pipes in Extensive Fills.

The settlement of the fill at the sides of a stiff pipe results in a relief of pressure in the fill itself, and an added load on the pipe. Above the pipe there exists a certain zone of earth which is compressed under a pressure greater than the hydrostatic earth pressure at that depth. The height of this "zone of disturbance" is given by the following conditions, as previously listed in Section II - 2 - A, equations (15), (18), and (19):

$$\frac{w}{u} = \frac{v}{4u} \; \frac{2\ln\frac{v}{u} + \left(\frac{u}{v}\right)^2 (2\mu^2 - 1) - 1}{\ln\frac{v}{u} + \mu \cdot \frac{u}{v} - 1} \qquad (6)$$

In this, $\mu = \frac{u_o}{u}$; the other symbols are as given in Fig. 3.*

* In this Figure $2b_o = \frac{\pi}{2} r_a$. This gives the length of the side of the square, and $u = \frac{b_o}{\tan \rho}$.

For any given value of $\frac{w}{u}$, there are two roots for $\frac{v}{u}$ from equation (6). Of these, the smaller is to be used, as may readily be seen from the boundary conditions $\frac{w}{u} = \infty$.

By assuming $\frac{v}{u}$ and μ one can compute the corresponding values of $\frac{w}{u}$, as has for example been done in Fig. 24 (p.71) for the case $\mu = 0$, i.e. $u_o = 0$.

Also, if for a given value of $\frac{w}{u}$ the corresponding value of $\frac{v}{u}$ is known, then, as shown in Section II - 2 - A, equation (14), the average specific vertical loading on the rigid pipe is:

$$\bar{q} = \gamma \cdot \nu \cdot \left[\frac{v}{u} \left(\frac{w}{u} - \frac{v}{2u}\right) - \frac{1}{2}\right] \tag{7}$$

This pressure is somewhat high when considered in the light of the discussion at the end of Section II - 2 - A.

If, from equation (6), $\frac{w}{u} < \frac{v}{u}$ then one must substitute $\frac{v}{u} = \frac{w}{u}$ into equation (7), since under these conditions the upper limiting value is reached.

In order to find the added pressure Δq due to the compressibility of the fill, one must subtract the hydrostatic earth pressure γ (w - u) from equation (7), and then multiply the result by $\pi/4$, as was shown in Section II - 2 - A.

The result is:

$$\Delta q = \gamma u. \quad \pi/4 \left[\frac{v}{u} \left(\frac{w}{u} - \frac{v}{2u}\right) - \frac{w}{u} + \frac{1}{2}\right] \tag{8}$$

In order to simplify practical computations, the values of $\frac{v}{u}$ have been computed from equation (6) as a function of the depth-of-cover condition $\frac{w}{u}$ for various embedment depths in stiff soils: μ = 0, 0.25, 0.5, 0.75 and 1.00. These have been substituted in equation (8) with the result that the added pressure on rigid pipes in extensive fills may be taken directly from Fig. 3.

The internal stresses in the pipe due to the added pressure Δq are found from the formulae of Figure 2, if instead of the crown pressure q, the added pressure Δq is substituted. The added stresses thus found must then be superimposed to the stresses found from Fig. 1.

(b) Pipes in Trenches

For rigid pipes in trenches there also exists a super-compressed earth zone, the extent of which, and the resulting added pressure, may be found from the theory of Section II - 2 - B. For practical purposes, the following closely approximate formulae suffice -- (compare Fig. 25, p.71):

The uniformly distributed specific vertical pressure is:

$$\bar{\bar{q}} = \gamma \left[\frac{b^2 - b_o^2}{2r_a} \cot. \rho + \frac{bt'}{r_a} . \Phi \right] \qquad (9)$$

where $b_o = \pi/4 . r_a$ (10)

and $t' = t_o - b_o - (b - b_o) \cot. \rho$ (11)

The numerical value of Φ may be taken from Fig. 2 for values of the function $x = \frac{t'}{b} . \Psi$, where Ψ is also given in Fig. 2 as a function of the angle of internal friction $\rho = \rho'$.

If formula (11) for t' becomes negative, then the following equation must be used in place of (9):

$$\bar{\bar{q}} = \gamma \frac{t_o - b_o}{2r} \left[2b_o + (t_o - b_o) \tan \rho \right. \qquad (12)$$

(upper limiting value of earth pressure when depth of cover is small)

The pressure $\bar{\bar{q}}$ of equation (9) becomes greater with increasing width of trench until it finally reaches, at great depths of backfill and a very wide trench width 2b*, the value $\bar{q}$ for extensive f lls as given by equation (7). This latter value of $\bar{q}$ then remains constant for all wider trenches ($b > b^*$).

For very rough computations of pipes in relatively narrow trenches, the following approximate formula will serve in place of equations (9) and (12):

$$\bar{\bar{q}} = \frac{b + r}{2r} . q$$

, where q is from equation (3), given graphically in Figure 2.

C. EXTERNAL AND INTERNAL WATER PRESSURE; DEAD WEIGHT

(a) External Water Pressure

The stresses in this case are obtainable from the formulae of Fig. 1 if the coefficients for the internal s resses are taken for $\rho = 0$, with t_o representing the height of the water table above the pipe centerline.

For soil that is submerged in water, the value of its density is $\gamma_u = (1-n)\ (\gamma_s - \gamma_w)$, where the symbols are as given in Section 1-A of this chapter. The pressure of the soil below the water table is computed as was done in Section 1-A. This pressure, and the pressure due to the water, act independently. The internal stresses due to the dry soil lying above the groundwater table may be found using the formulae of Fig. 2 by assuming the dry soil to act as a uniformly distributed surcharge.

(b) Internal Water Pressure

The solution may be taken from Fig. 1 as follows: Choose the stress coefficients for $\rho = 0$ and substitute them with reversed sign into the formulae for M and N; the internal radius (r_i) must be used in place of the outer radius (r_a).

(c) Dead Weight of Pipe Itself

The internal stresses due to the dead weight G of the pipe per unit of the length may be taken from Fig. 6. The moments are proportional to those for internal water pressure while the normal stresses are not.

D. SURFACE LOADS

The action of single loads (wheel loads) may be computed using Boussinesq's method. The specific pressure

$$p = \frac{3P}{2\pi R^2} \cos \beta \quad \text{(symbols on Fig.6)} \qquad (14)*$$

is taken as uniformly distributed for normal cases, and any pressure due to impact is neglected.

The computation of internal stresses follows the formulae of Fig. 2, with pressure p substituted in place of "q".

For the case of a distributed surface load, see Section I, Sect. 3, part B.

---

* This gives the unit pressure on a plane normal to the radius from P.

2. EFFECT OF THE BEDDING CONDITIONS

In the previous section, it was assumed that the pipe was supported on a line reaction. In order to analyse the actual reaction conditions, an imaginary single vertical load (-Q), equal in magnitude but opposite in direction to the linear reaction of the previous section, is assumed to act on the sole of the pipe (see Figure 4). The inner stresses resulting from the reaction conditions on the pipe due to this fictitious load are then solved. By superimposing these stresses upon the internal stresses resulting from the linear reaction of the previous section the internal stresses due to the actual reaction conditions are arrived at. In this process the linear reaction Q and the opposite fictitious load (-Q) cancel each other.

The linear reaction is equal to the sum of the vertical components of the external loads. Its value (R) may be taken from Fig. 4 for external earth and water pressure; for all other types of loads dealt with so far, it is easily found. The sum of the vertical components of <u>all</u> acting loads is designated by Q.

In the case of the water table being considerably above the pipe center-line, it is possible that the reaction will be negative due to uplift. (Compare coefficients for R in Fig. 4). It is then, according to the theory of elastic embedment, replaced by radial earth reactions proportional to cos α acting on the upper half of the pipe. The internal stresses for such a reaction condition may be computed according to Section II - 4 - B. In order for the pipe to remain in equilibrium, the total resulting uplift must not exceed the upper limiting value of the earth loading (see equation (17), Chapter I).

Boundary Case 1 : Radial Reactions

Normally the sum Q of all vertical load components will be directed downward. The resulting reactions on a rigid pipe are then directed nearly radially on to the pipe, according to the laws of elastic embedment (compare Section II - 3 - B). This is shown in Fig. 28(p. 78)*. For this case, the added stresses due to the reaction conditions are given in Fig. 4.

Boundary Case 2 : Vertical Reactions

It is possible that due to unusual embedment conditions (strength of soil in horizontal direction much less than in vertical direction, squeezing out of the material under the pipe) tangential reaction prsssures may be set up.

---

* Not required. Reaction pressure is also shown in Fig. 4.

If these are present, their magnitude cannot become larger than the vertical direction of the reaction pressures allows. Since, as may be seen in Section II - 3 - B, the reaction pressures are determined to a first approximation by the radial displacements of the pipe, then the distribution of the vertical reactions will also depend chiefly on the radial displacements. If, as before (Sect. II - 3 - B), the reaction pressures are determined from the radial displacements for materials with constant bedding coefficient (dense material) or with lineally increasing bedding coefficient (loose material), but with the direction of the reactions maintained as vertical, then the reaction pressures shown in Figure 6 result. In order to simplify the computation of the effect of embedment in loose material, the circular arc was in this case replaced by a parabola. This simplification causes no noteworthy inaccuracy. The additional stresses which result from bedding the pipe on dense, as well as loose, material with resulting vertical reaction pressures may be taken from Figure 6. By combining Figures 4 and 6, the effect of several different bedding conditions may be dealt with.

3. INFLUENCE OF THE CURVATURE OF THE PIPE WALL ON THE INTERNAL STRESSES

The assumption of a linear variation in internal stresses is sufficiently accurate for pipe walls with such ratios of thickness to radius of curvature as occur in most normal cases. In order, however, for the previous computations to be basically correct, extra forces M^*, N^* must be added to the inner forces as already determined, so that the following conditions are satisfied:

1. The axis of the pipe suffers no change in length under pure bending.
2. The pipe remains perfectly circular under loading of its walls by normal forces only (e.g. internal fluid pressure).

Condition 1 is fulfilled if the fibre deformations at the outer and inner pipe surfaces become equal under bending alone. The internal stresses are figured per unit length of pipe, with F being the area and W the section modulus per unit length of pipe. The outer and inner radii of the pipe are signified by r_a and r_i respectively, and the wall thickness by δ.

$$\frac{M}{E \cdot W} r_a \cdot d\varphi - \frac{N^*}{E \cdot F} r_a \cdot d\varphi = \frac{M}{E \cdot W} r_i \cdot d\varphi + \frac{N^*}{E \cdot F} r_i \cdot d\varphi$$

from which

$$N^* = \frac{M \cdot F}{W} \cdot \frac{r_a - r_i}{r_a + r_i} = \frac{3M}{r} \tag{15}$$

Condition 2: If the pipe is loaded by pure normal forces, then it must remain truly circular in cross-section. The outer and inner fibres undergo equal deformations.

$$r_a \left(\frac{N}{E \cdot F} - \frac{M^*}{E \cdot W}\right) = r_i \left(\frac{N}{E \cdot F} + \frac{M^*}{E \cdot W}\right)$$

from which

$$M^* = \frac{N \cdot W}{F} \cdot \frac{r_a - r_i}{r_a + r_i} = N \frac{\delta^2}{12r} \tag{16}$$

Using the sign convention of Figure 6, these additional forces N*, M* are always of the same sign as the forces M, N which cause them. The maximum stresses found with due consideration of the above added forces are somewhat smaller than those given by the Theory of Elasticity. One is referred to special investigations for the analysis of extraordinarily thick-walled pipes. (See ref. 119). The solution given here, and plotted in Figure 5, is by Lamé, and gives only the practically important maximum stress on the inside of the thick-walled pipes due to internal and external pressures.

4. SIMPLIFIED COMPUTATION OF RIGID PIPES

In Figure 6 the most important formulae for ordinary pipe investigations are summarized. These formulae are simplified in that the depth of cover over the upper pipe half is taken as constant. Furthermore, the active side pressure on the lower pipe half is assumed as acting in its horizontal (limiting) direction, and as vanishing on the lowest quarter of the pipe circumference. At this point the lateral pressure is always very small; thus the assumption results in no important inaccuracy.

In further simplification it may be noticed that the coefficient for the inner moment at the crown will, with reversed sign, give quite accurately the moment at the side. Those formulae spoken of previously for other cases of loading were entered in Figure 6 without change.

Computation of Stresses: The commonly adopted sign convention for inner stresses (Moment M, Normal stress N) has been used in this work, as may be seen from Figure 6. If the internal stresses are considered per unit of length of the pipe, then the maximum stresses for the slice of pipe are given by

$$6 = -\frac{N}{F} \pm \frac{M}{W} = -\frac{N}{\delta} \pm \frac{6M}{\delta^2}$$

Upper sign: Outer circumference . Tension stresses positive

5. STRESSING OF ELASTIC PIPES

The radial deformations y of the wall of a loaded pipe produce passive pressures

$$P_1 = k_y$$

Herein k is the bedding coefficient which, as was shown by the investigations of Chapter III, may be taken as constant for pipes laid without slope in extensive fills. The value of the bedding coefficient may be estimated from the following formula, given in Section II - 2:

$$k = \frac{2\ E_1}{3\ r_a} \left(\gamma t_o + c_1 \right) \tag{17}$$

where E_1 and c_1 are the constants for a soil compression test with lateral deformation restrained (Fig. 21 ;. 59)*. Further methods for the determination of the bedding coefficient arise out of Sect. II - 1, where its dependence on various physical and geometrical influences is discussed. E_1 is a dimensionless constant, c_1 is a stress.

> At this point it was also shown that the tangential displacements of the wall of a loaded pipe produce shearing forces on its outer circumference; however, in comparison to the passive pressures resulting from radial deformations they are very small, and consquently may be neglected. The investigation of the elastic bedment may therefore be narrowed down to radial forces.

The loading of rigid pipes (Sections I - 1 and I - 2 of this Chapter) forms the basis for the investigation of the loading of elastic pipes.

> As a rough approximation, the pressure on rigid pipes under wide and high fills may be estimated by multiplying those pressures found without consideration of the effect of deformations (equations (1) & (2) of this Chapter) by the following pressure-concentration factor:

$$\chi = \frac{5}{3} \tag{18}$$

---

* This is the customary confined compression test for the soil, showing compressive strain plotted against pressure.

The stressing of rigid pipes due to the shearing forces T acting on the pipe circumference is now dealt with by itself, as these are not noticeably influenced by the pipe deformations. This computation is done most practically in an approximate form, as a more exact solution gives no noteworthy differences despite formidable trouble.

The maximum shear stress exists approximately at the upper quarter point of the pipe circumference, its value being:

$$\tau_{max} = -\gamma\left(t_o - \frac{r}{\sqrt{2}}\right)\frac{\sin\rho}{1+\sin\rho}$$

(symbols in Fig. 1)

If the variation in depth of cover over the upper half of the pipe is neglected, as may be done since τ quickly diminishes at the crown and sides of the pipe, then at any point located by α:

$$\tau_\alpha = \gamma\left(t_o - \frac{r}{\sqrt{2}}\right)\frac{\sin\rho \cdot \sin 2\alpha}{1+\sin\rho} \qquad (19)$$

Using this value, the approximate solution yields the following inner stresses:

Upper half of pipe:

$$M_a = \frac{2\,r^2 \cdot \tau_{max}}{3}\left[\frac{1}{\pi} - \frac{1}{8} - \frac{\cos\alpha}{3\pi} - \frac{\sin^2\alpha}{2}\right] \qquad (20)$$

$$N_a = -2\,\frac{r \cdot \tau_{max}}{3}\left[2\sin^2\alpha + \frac{\cos\alpha}{3\pi} - 1\right] \qquad (21)$$

Lower half of pipe:

$$M_a = 2\,r^2\,\tau_{max}\left[\frac{1}{3\pi} + \frac{1}{8} - \frac{\cos\alpha}{9\pi} - \frac{\sin\alpha}{3}\right] \qquad (22)$$

$$N_a = \frac{-2\,r \cdot \tau_{max}}{3}\left[\frac{\cos\alpha}{3\pi} + \sin\alpha\right] \qquad (23)$$

These inner stresses are to be superimposed to results of the investigation of elastic, radially loaded pipes, which follows.

The radial pressures of rigid pipes (Formulae 53, 54 of Section II - 3 - A) and the corresponding radial reaction pressures (Section II - 3 - B) determine the limits for the computation of the loading of elastic pipes.

The equation of the influence line for the determination of the passive pressures on elastic pipes is, from Section II - 4 - A - e:

$$p_1 = k \cdot y = \frac{\sqrt{a^2 - 1}}{2r} \left(\frac{2u \cdot v}{a^2} + U \cdot \text{sh}\, u\varphi \cdot \sin v\varphi - V \cdot \text{ch}\, u\varphi \cdot \cos v\varphi \right) = K \cdot r^3 \cdot \eta \qquad (24)$$

where $a = \sqrt{1 + \frac{r^4 \cdot k}{B}}$, $B = \frac{m^2}{m^2 - 1} \cdot E \cdot J$, $u = \sqrt{\frac{a - 1}{2}}$, $v = \sqrt{\frac{a + 1}{2}}$.

$$U = \frac{u \cdot \text{sh}\, u\pi \cdot \cos v\pi - v \cdot \text{ch}\, u\pi \cdot \sin v\pi}{a(\text{sh}^2 u\pi + \sin^2 v\pi)},$$

$$V = \frac{u \cdot \text{ch}\, u\pi \cdot \sin v\pi - v \cdot \text{sh}\, u\pi \cdot \text{cis}\, v\pi}{a(\text{sh}^2 u\pi + \sin^2 v\pi)}$$

E = Modulus of elasticity of pipe material

m = Poisson's number of pipe material (the lateral deformation constant)

J = Moment of inertia of pipe wall per unit of length of pipe.

In Figure 7 this influence line is drawn for an iron pipe ($E = 2{,}000{,}000$ kg/cm^2, $k = 10$ kg/cm^3) of internal diameter = 66 cm., and wall thickness = 1 cm. This influence line holds good for pipes of any material or dimensions, as long as they have the same deformation characteristics, i.e.

$$\frac{r^4 K}{E \cdot J} = 71$$

For computation of the passive pressures on an elastic pipe, the influence line for the earth loading must first be evaluated considering the pipe as rigid. In this computation, all the forces acting on the whole pipe circumference must be considered, including active loads and bedding reaction pressures.

The negative values of the deformation y arising out of this evaluation mean a reduction in the pressure on the pipe p due to the elasticity of the pipe wall.

The resulting additional loads are to be superimposed on the loading of a rigid pipe, with the result that the required pressure on an elastic pipe is found. The greater the elasticity of the pipe, the less will be the pressure on its crown. Should the resulting total vertical pressure be less than the limiting value (14) given in Section I - 2 - A - a, then this limiting value is to be used in the pipe analysis.

The evaluation of the influence lines shows a change in the pressure distribution whereby a decreasing stiffness of pipe wall brings about increasing side-pressures, which results in a lessening of stresses in the pipe. A numerical example (compare next section) clearly shows the advantageous effect of an elastic pipe wall. This advantageous effect of the passive side-pressure may only be realized, however, through careful placing of the fill material, and if the long-time elasticity of the fill material is not adversely affected by strong vibrations or varying moisture conditions.

The computation of the internal stresses resulting from the loading of an elastic pipe follows the method of Section II - 4 - A - f on the basis of the generally applicable influence lines (Figure 8):

$$M_1 = \frac{r}{2\pi} \left(\varphi \cdot \sin\varphi + \frac{\cos\varphi}{2} - 1 \right) = r\eta_1 \qquad (25)$$

$$Q_1 = \frac{1}{2\pi} \left(\varphi \cdot \cos\varphi + \frac{\sin\varphi}{2} \right) = \eta_2 \qquad (26)$$

$$N_1 = \frac{1}{2\pi} \left(\varphi \cdot \sin\varphi + \frac{\cos\varphi}{2} \right) = \eta_3 \qquad (27)$$

A single evaluation of the ordinates for these influence lines (equations (25) to (27)) suffices for the analysis of pipes of all dimensions and the most varying radial loadings, whether these arise due to earth pressure or outer or inner water pressure. Due to the deformation conditions of the pipe, the radial direction of the bedding reactions is usually the best to use; the distribution of these may at times be assumed, and in the evaluation of the influence lines (equations (25 to (27)) they must be considered as external forces. By using the influence lines as found, (equations (25) to (27)) it is possible to complete in parts the analysis of pipes with an assumed distribution of radial loads, and in a time comparable to that required using present methods of investigation.

To complete this analysis it is necessary to include the effect of the shearing forces acting on the upper half of the pipe. These forces, covered by equations (20) to (23), are not influenced by the elasticity of the pipe. The vertical components of these shearing forces, which are required to determine the resulting bedding reactions, are approximately equal to half the vertical components of the normal forces.

If the computation is carried out for a condition in which the pipe breaks, then at the point of maximum shearing stresses (upper quarter of pipe) these shearing stresses are greatly reduced by the breaking deformation. In the computation for this failure condition, the effect of the shearing forces on the pipe wall may then be neglected. The computation of the internal stresses is then concerned wholly with the general influence lines, Fig. 8.

The above method of analysis assumes ideal bedding conditions which will actually only be realized if the conduit is laid on a bed of fine-grained material which matches itself exactly to the underside of the pipe surface; furthermore the fill under and alongside the pipe must be of dense material well tamped in, and with no cavities left. This lateral condition can never be realized with certainty in narrow trenches, which explains the reason for not assuming a passive side-pressure in such cases. In contrast, a complete embedment of the pipe in embankments may be produced by careful backfilling. This brings with it a large increase in safety against failure, as may be shown mathematically. The literature (30, 33, 34)* contains many examples where neglect in observing the above conditions has led to pipe failures. Also it was noticed that numerous cases of pipe damage occurred when the pipe was laid on the original soil instead of being laid on a bed of sand. If the conduit is laid on a poorly pre-formed bed and the backfill is not properly tamped into the narrow angle beneath the pipe, then the pressure concentration under the sole of the pipe will never be evened out after backfilling is completed. (Compare Chapter III - Tests).

---

* These refer to Bulletins Nos. 31, 36 and 47 of the Iowa Engineering Experimental Station.

The analysis of a pipe laid on a concrete sole may be carried out by first considering the pipe as rigid and by using values of the bedding coefficient that vary in steps. The computation is similar to that given in Section II - 4 - B for a partly embedded pipe.

According to the tests of Chapter III, the assumption of using a bedding coefficient value that increases directly proportionally to the depth for the analysis of embedded pipes is normally less accurate than the assumption of a constant bedding coefficient.

For the analysis of small conduits, which do not warrant an exact computation of the pressure distributions, an approximate method as given in Section II - 2 may be used to determine the effect of the elasticity of the soil and pipe.

6. EXAMPLES OF PIPE ANALYSIS

A. PIPES IN EXTENSIVE FILLS

In order to clarify the method of analysis developed herein an example follows in which the state of stress of the iron pipe used in the tests of Chapter III under 6 meters of fill, is investigated.

Iron Pipe

Depth of fill above pipe axis:	t_o	= 600 cm.
Average radius:	r	= 33 cm.
Outer radius:	r_a	= 33.5 cm.
Modulus of elasticity:	E	= 2,000,000 kg/cm^2
Bedding angle:	φ_o	= 45°

Fill Material

Sand, pressure diagram as in Fig. 21. $E_1 = 70$, $c_1 = 6$ kg/cm^2

Unit weight: $\gamma = 1.85$ t/m^3 = 0.00185 kg/cm^3

Angle of internal friction $\varphi_o = 35°$

1. Rigid Pipe

First the distribution of the active pressure was computed according to Equations (1) and (2) of this chapter, using the figures listed above, and the results multiplied by the concentration factor $\chi = \frac{5}{3}$ for reasons given in the previous sections. The result , being the nearly correct pressure distribution for the pipe considered as rigid at the present, was plotted (σ_s)over the left half of the pipe in Fig. 9.

The vertical components R of this normal earth pressure are according to Figure 4:

$$R = \gamma \cdot r_a(t_o \cdot v_u + r_a \cdot \bar{v}_u)$$

The coefficients v_u and $\bar{v}_u$ are read from the applicable curves of Figure 4 (upper right quarter) for the value of ρ as given.

The vertical components $\bar{Q}$ of the total earth pressure on the rigid pipe is, because of the pressure concentration, equal to

$$\bar{Q} = \chi \cdot R$$

As the computation which follows takes no account of the shearing forces, then in the evaluation of the bedding reactions a value of only $\frac{2}{3}$ or R should be used. In this example, the bedding was considered to be on loose material, and the bedding reactions for this condition were computed from the proper formulae of Figure 4 (with $\alpha_0 = \varphi_0 = 45°$). The result is plotted in Fig. 9 on the left half of the pipe ($\sigma_{s,\alpha}$).

The pipe circumference was then divided into 36 parts λ, and the distributed earth pressure was converted into single forces P concentrated at the division points using the trapezoidal formula. For instance, the force P_n acting at division point n is:

$$P_n = \frac{\lambda}{6} (\sigma_{n-1} + 4\sigma_n + \sigma_{n+1})$$

Finally, using these single forces, the general influence lines of Fig. 8 were evaluated, and the moment and normal force determined for each of the 36 points. These values are also plotted on the left side of Figure 9. The shearing force Q, is of negligible importance for this case. In the critical section, occurring at the pipe sole, the following forces exist: M = 402.5 cm. kg/cm., N = 23 kg/cm. Thus, if the pipe is considered as rigid the maximum stress turns out to be 2440 kg/cm^2. In the next analysis it will be shown that due to the flexibility of the iron pipe this stress is greatly reduced.

2. Elastic Pipe

The value of the bedding coefficient at a depth of 6 m. is, according to the assertions of the previous section:

$$K = \frac{2\,E_1}{3\,r_a} (\gamma t + c_1) = 10 \text{ kg/cm}^3$$

Also, for this pipe, the following stiffness characteristic applies:

$$\frac{r^4 K}{B} \approx \frac{r^4 K}{E J} = 71$$

For this case the influence line for the radial deformations y and for the added pressure of bedding $P_1 = k.y$ were evaluated and the results plotted in Fig. 7 as already stated in the previous section. These influence lines are then evaluated for the earth pressures and reaction pressures of the rigid pipe which are plotted on the left side of Fig. 9.

In the evaluation of these influence lines the circumference was divided into 36 parts and the earth pressure reduced to single forces acting at the division points, as in the example just previous.

The deformations, y, are made up of two parts: the first, and greater part $y_s = \Delta_{s\ u.} \cos \varphi$ is the result of a vertical displacement of the whole pipe, presently considered as rigid (compare Section II - 3); the second, lesser part, is a result of the bending of the supposed absolutely rigid pipe due to the elasticity of the pipe wall. A knowledge of this second part y of the radial displacement of the pipe wall suffices for the computation of the effect of the pipe elasticity in evening-out the pressures. This is arrived at from the influence line for y in Fig. 7 by evaluating it for all active forces and reaction pressures acting on the rigid pipe.

The elastic line for y was entered on the right side of Fig. 9. The elastic deformation y of the pipe wall is tied in with a change in bedding pressure: $p = k.y = 10.y.$ These pressure changes p are algebraically added to the pressure σ_s acting on the so-called rigid pipe, and the result is the loading σ_e on an elastic pipe, which may be seen on the right side of Fig. 9.

The further analysis may follow two courses:

1. The internal stresses are solved with the aid of the influence lines, Fig. 8. for the rigid pipe, using, however, the loading σ_e of the elastic pipe.

2. The influence lines, equations (88) - (90), Chapter II, for an elastic embedded pipe may be evaluated using the loading σ_s of the rigid pipe.

Both methods lead to the same result. As a rule it will be simpler to use the generally applicable influence lines of Fig. 8, as then only the influence line for the embedment pressure p on the elastic embedded pipe need be determined, which line differs from the influence line for the deformation y only in scale.

The result of the analysis is plotted on the right side of Fig. 9. The elasticity of the pipe causes a noteworthy evening-out of the pressure, as has been observed in numerous tests (53). At the sole cross-section the value of the moment M is 103.9 cm.kg/cm. and of the normal force, 31.8 kg/cm. The maximum stress in the pipe reaches 655 kg/cm^2, i.e., about 1/4 of the stress in the rigid pipe.

If the analysis were carried out using the lesser bedding coefficient of $K = \frac{1}{2}$ kg/cm^2, which value was found in the tests of Chapter III under the conditions existing there, then the s de pressure on the above iron pipe would only increase by about 1/4; the maximum stress, however, would already be about 1/3 less than that of the rigid pipe. One may check this from the deformation line, Fig. 63*, which serves also as influence line for the bedding pressure. Once the pressure distribution on the elastic pipe is thus determined, the internal stresses follow from an evaluation of the influence lines of Fig. 8.

B. CONDUIT IN A TRENCH

Figure 10 shows a cement pipe of 60 cm. internal diameter which is laid on a concrete base in a trench 1.1 m. wide with a fill of 4.0 m. above its axis. Further details may be seen in the figure.

The comparatively thick walled pipe may be considered as rigid. From equation (9) of this Chapter the uniformly distributed vertical pressure is given by

$$q = \gamma \left[\frac{b^2 - b_o^2}{2 \cdot r_a} \cdot ctg.\, \rho + \frac{b\, t'}{r_a} \cdot \Phi \right]$$

Herein, with reference to Figure 10:

$$b_o = \pi/4 \cdot r_a = 27.5 \text{ cm.}$$

$$t' = t_o - b_o - (b - b_o)\, ctg.\, \rho = 333 \text{ cm.}$$

From Figure 2, for $\rho = \rho' = 35°$, the value of the function $\Psi = 0.190$. Then for $x = \frac{t'}{b} \cdot \Psi = 1.15$, the value of Φ is 0.59 from this same figure.

Substituting these values in the above equation

$$q = 0.63 \text{ kg/cm}^2.$$

As the pipe rests on a concrete bed, it may be assumed that the distribution of bedding pressures is dependent on a constant bedding coefficient. From Figure 4 the value of the bedding-reaction is

---

* This refers to an experimental measurement of the deformation of a circular iron pipe.

$$q_1 = \frac{2\ Q \cos \alpha}{r_a(\sin 2\alpha_o + 2\alpha_o)} = 0.91 \cdot \cos \alpha \quad \text{in kg/cm}^2$$

From Figure 2, with the pipe considered as supported by a line-reaction, the values of the internal forces at the sole, where the maximum stressing usually occurs are

$$M = -0.587 \cdot r \cdot r_a \cdot q \qquad N = 0.106 \cdot r_a \cdot q$$

From Figure 4, with $Q = 2r_a \cdot q$, the effect of the action of a distributed bedding reaction is found to be

$$M = 0.365 \cdot r \cdot r_a \cdot q \qquad N = 0.414 \cdot r_a \cdot q$$

By superposition, the result is:

$$M = -0.222 \cdot r \cdot r_a \cdot q = -166 \text{ cm.kg/cm.}$$

$$N = 0.520 \cdot r_a \cdot q = 12.0 \text{ kg/cm.}$$

Due to the curvature of the pipe wall, the following additional forces (taken from Fig. 6) must be considered:

$$M^* = N \cdot \frac{\delta^2}{12\ r} = \frac{11.7 \times 5^2}{12 \times 32.5} = 0.76 \text{ cm. kg/cm}$$

$$N^* = \frac{3\ M}{r} = \frac{-3 \times 166}{32.5} = -15.3 \text{ kg/cm.}$$

The effect of the curvature of the pipe wall is not too serious for the case under consideration; it increases the maximum stress by 7%. This stress is

$$\sigma_{max} = -\frac{M + M^*}{W} - \frac{N + N^*}{F} = -45.3 \text{ kg/cm}^2$$

A reduction of loading due to passive side-pressures is not to be considered for this relatively rigid cement pipe.

7. GENERAL REMARKS ON DESIGN

A. STRENGTH AND ELASTICITY OF PIPE MATERIALS

The properties of pipe materials vary in a wide range; therefore no generally applicable values may be given. The design and construction of important conduits should in all cases be based on special test results. The summary which follows has only value in that it orients one on the approximate size of those properties which are of first importance in the problem of the safety against failure of embedded pipes.

The resistance of mild steel pipes is endangered by large deformations, as soon as the stress passes the yield point of steel, regardless of whether this stress is the result of bending or of internal pressure. In contrast to this, all the other materials listed in the summary have only about one-half the strength in resisting hoop tension due to internal pressure that they exhibit in resisting flexural tension stresses.

The flexural tension strengths given for centrifugally cast concrete and cement pipes is limited by the formation of cracks. The carrying capacity of these types may be increased to far beyond the crack-producing loads by using reinforcing, but there is always the danger of the reinforcing iron rusting.

B. FACTORS OF SAFETY

As a rule, the failure of a conduit which does not carry any internal pressure does not bring with it any unremediable danger; one can therefore satisfactorily use a factor of safety of about 1.5 in a careful computation of internal stresses due to bending loads. This means that the allowable stresses may be allowed to reach 2/3 of the maximum values found for flexural strengths in actual tests.

On the other hand, the failure of a pressure line means great danger; in this case one should not use less than a twofold factor of safety. In other words, the stresses due to internal pressure should not exceed half the experimentally determined hoop-tension strengths. These latter strengths are, for heavy construction materials, about half of the flexural tension strengths as given in the table which follows.

Type of pipe	Flexural Tension Strength kg/cm^2	Modulus of Elasticity t/cm^2	Special Suitability
Mild Steel Pipes	2400 (minimum yield point)	2000	Pressure Conduits
Centrifugally Cast Pipes (Iron)	4000	1400	Pressure Conduits
Ordinary Cast-Iron Pipes	2000	1200	Water Mains
"Eternit" Pipes	350	250	Lines with Limited Internal Pressure
Stone Block Pipes	50-250	400	Chemically Active Water and Soil
Impregnated Cement Pipes	100-150	300	Chemically Active Water and Soil
Centrifugally Cast Concrete Pipes	70 (crack-formation)	350	Heavily Loaded Conduits
Normal Cement Pipes	40-110	300	Pipes Without Internal Pressure
"Prodorit" Pipes	80	300	Chemically Active Water and Soil
Clay Pipes	30-140	120	Drains of Small Diameter. Chemically Active Water and Soil

Fig. No. 1 Translated Words -

Earth over filling: Specific Weight , inner friction
angle natural angle of repose =

Upper half pipe Upper half pipe

Lower half pipe Lower half pipe

Influence of the pipe radius r
1000 fold coefficient values.

Influence of the over filling
height to 1000 fold coefficient
values

Crown Abutment Sole

Moment

Normal

COMPUTATION OF WIDE OVER FILLED PIPES. LINE SUPPORT

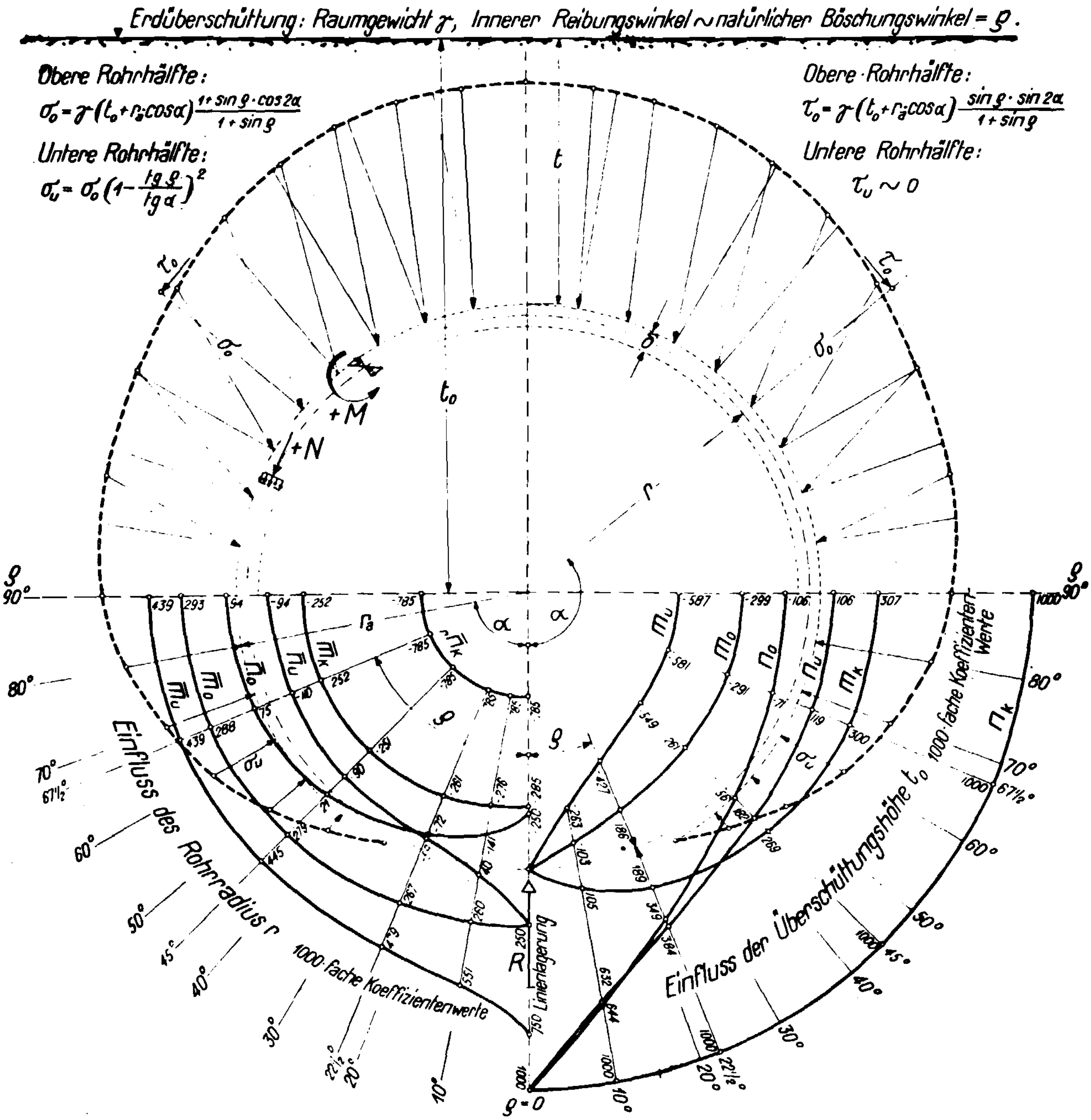

Scheitel: $\alpha = \pi$.

Moment: $1000\,M = \gamma \cdot r \cdot r_a \,(r_a \cdot \bar{m}_o + t_o \cdot m_o)$

Normalkraft: $1000\,N = \gamma \cdot r_a \,(r_a \cdot \bar{n}_o + t_o \cdot n_o)$

Kämpfer: $\alpha = \frac{\pi}{2}$.

$1000\,M = \gamma \cdot r \cdot r_a \,(r_a \cdot \bar{m}_k + t_o \cdot m_k)$

$1000\,N = \gamma \cdot r_a \,(r_a \cdot \bar{n}_k + t_o \cdot n_k)$

Sohle: $\alpha = 0$.

$1000\,M = \gamma \cdot r \cdot r_a \,(r_a \cdot \bar{m}_u + t_o \cdot m_u)$

$1000\,N = \gamma \cdot r_a \,(r_a \cdot \bar{n}_u + t_o \cdot n_u)$

Berechnung von weit überschütteten Rohren. Linienlagerung

FIG. 1.

Fig. No. 2   Translation:

Trench filling: Specific Weight
Inner friction angle
Wall friction angle ' =

Crown Pressure

from diagram for

from diagram for

' = = inner friction angle

Crown:

Abutment:

Sole:

COMPUTATION OF TRENCH CONDUITS. LINE SUPPORT.

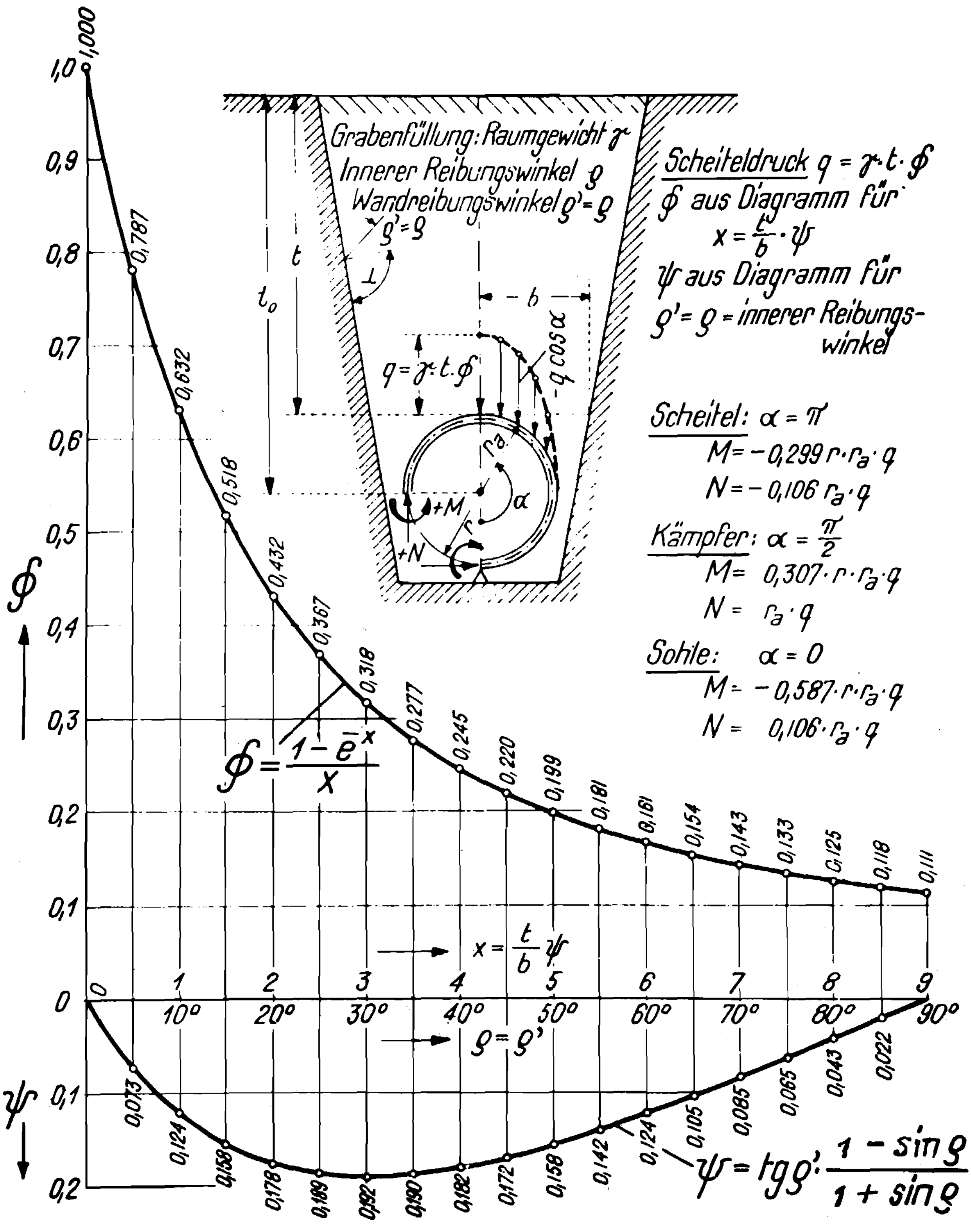

Berechnung von Grabenleitungen. Linienlagerung

FIG. 2

Fig. No. 3.

Upper limit value

SUPPLEMENTARY PRESSURE ON RIGID PIPE, DUE TO COMPRESSIBILITY OF THE FILLING.

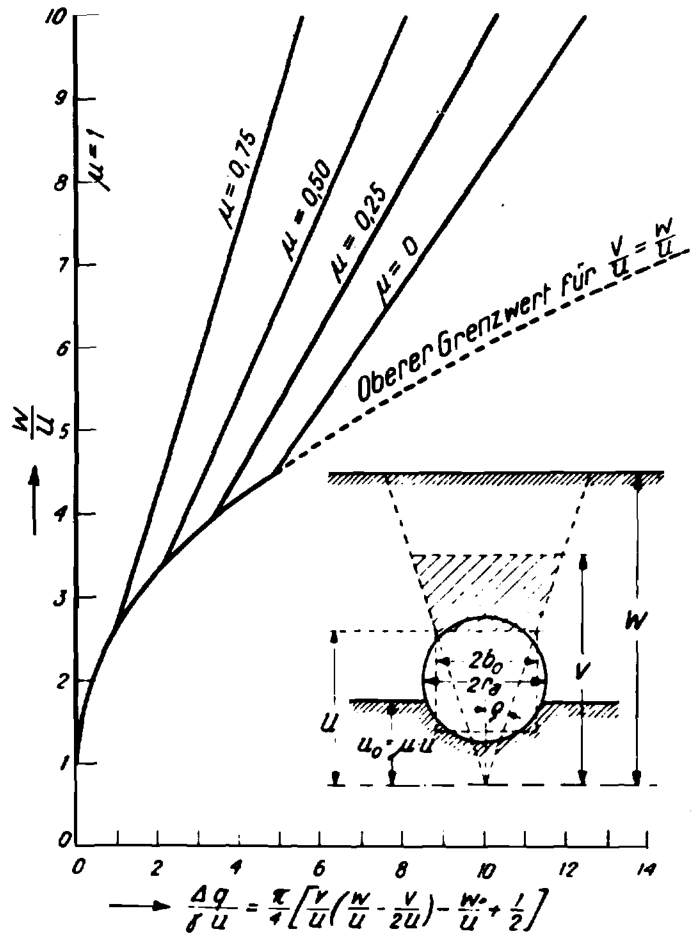

Zusätzdruck Δq auf starre Rohre, infolge Zusammendrückbarkeit der Schüttung

FIG. 3

Fig. 4.

Earth over filling: Specific Weight , inner friction angle natural angle of repose = .

Q: Vertical component of the active load.

Vertical component of the earth load

Support on firm material

Support on loose material

Crown:

Abutment:

Sole:

Moment:

Normal Force:

Vertical Components of the earth loading (Fig.66) in dependence of the friction angle . (Curves on the upper right quarter).

Inner forces due to radial distribution of the support reactions, in dependence on the support angle .

Support on firm material. (left curves)

Support on loose material (right curves)

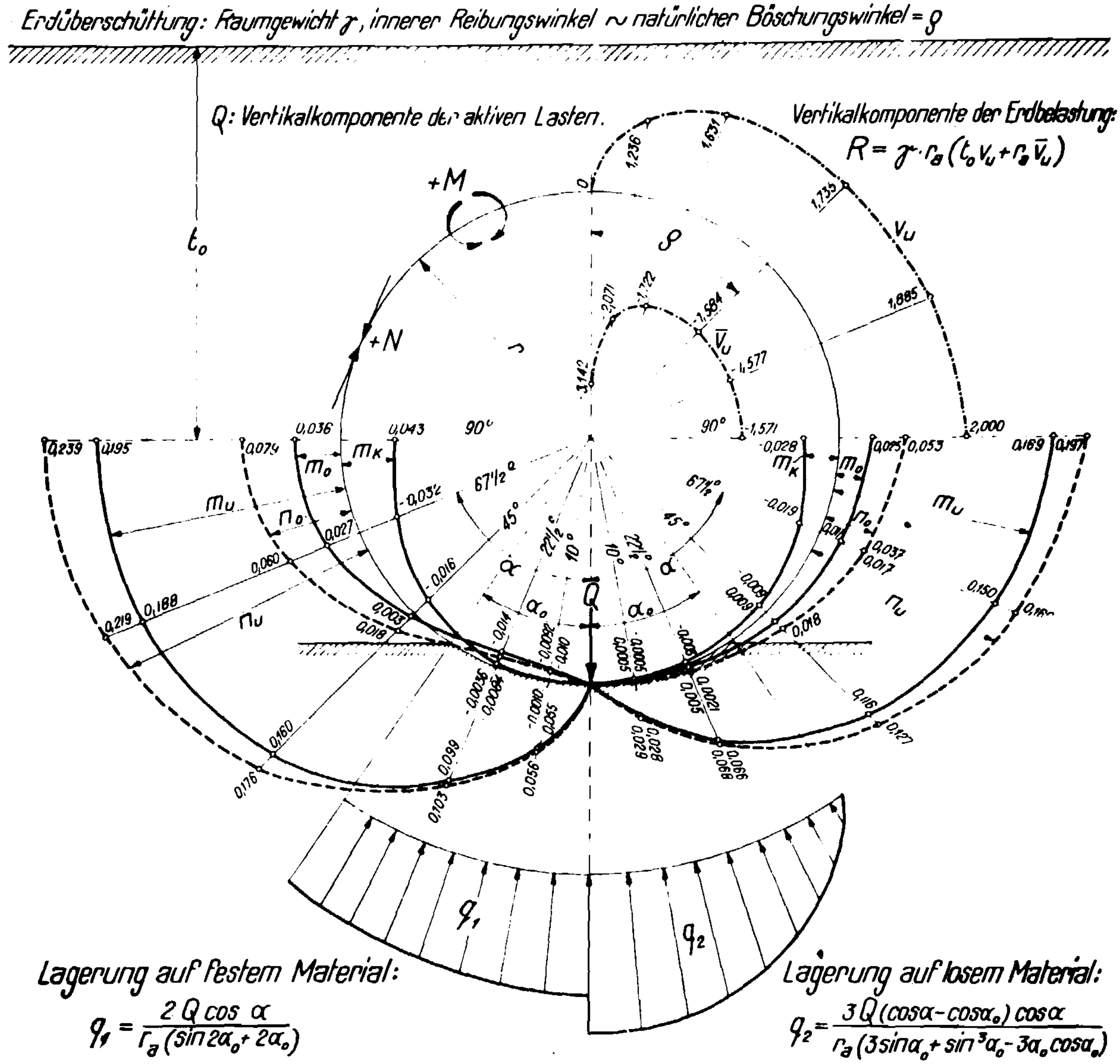

	Scheitel: $\alpha = \pi$	Kämpfer: $\alpha = \frac{\pi}{2}$	Sohle: $\alpha = 0$.
Moment:	$M_o = m_o \cdot r \cdot Q$	$M_K = m_K \cdot r \cdot Q$	$M_u = m_u \cdot r \cdot Q$
Normalkraft:	$N_o = n_o\, Q$	$N_K = 0$	$N_u = n_u \cdot Q$

Fig. 69. Vertikalkomponente der Erdbelastung (Fig. 66) in Abhängigkeit vom Reibungswinkel ϱ. (Kurven am oberen Viertel rechts)
Innere Kräfte infolge Verteilung radialer Auflagerreaktionen, in Abhängigkeit vom Auflagerwinkel α_0.
Lagerung auf festem Material (Kurven links). Lagerung auf losem Material (Kurven rechts)

FIG. 4

Fig. 5.

(Tension stress positive)

MAXIMUM STRESS, ACCORDING TO LAMÉ, AT THE INNER SIDE OF THICK-WALLED PIPES.

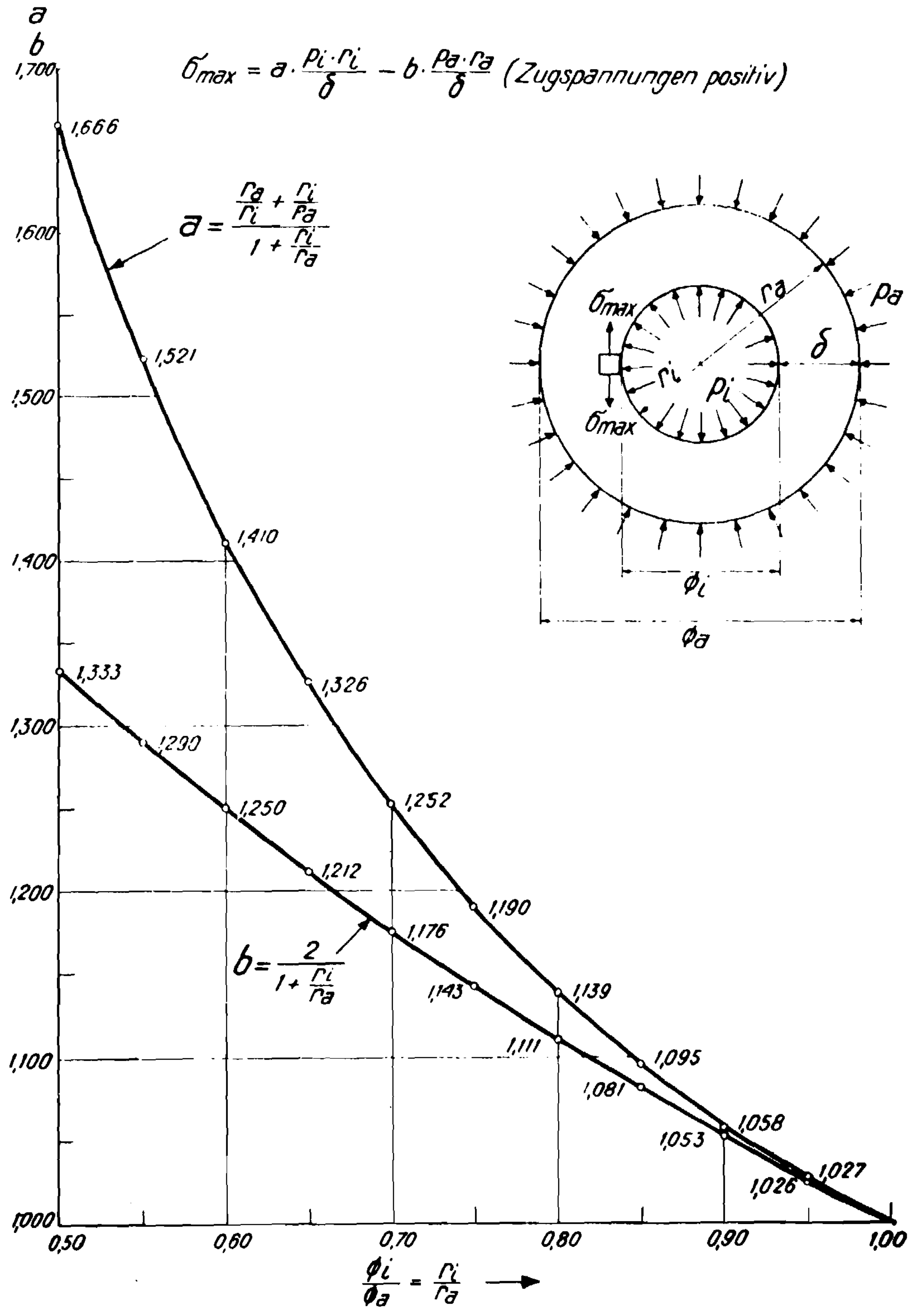

Maximalspannung, nach *Lamé*, an der Innenseite dicker Rohrwandungen

Fig. 5

Fig. 6

Earth over filling: Specific Weight
inner friction angle natural
angle of repose .

Stress condition according to
Rankine for large overfilling height

Crown:

Abutment:

Sole:

Coefficients for the present authoritative support angle

Support on firm material

Support on loose material

Pipe in wide filling

Pipe in Trench

Load increases due to stronger compressibility of wide filling are to be kept in mind.

Support on firm material.

Support on loose material.

Friction angle on the trench wall.

Formulas and coefficients for the simplified pipe computations.
Inner forces due to distribution of the vertical reaction, in dependence on the support angle is for rigid pipe still to be increased by the supplementary pressure (Fig. 5 , due to the compressibility of the filling.

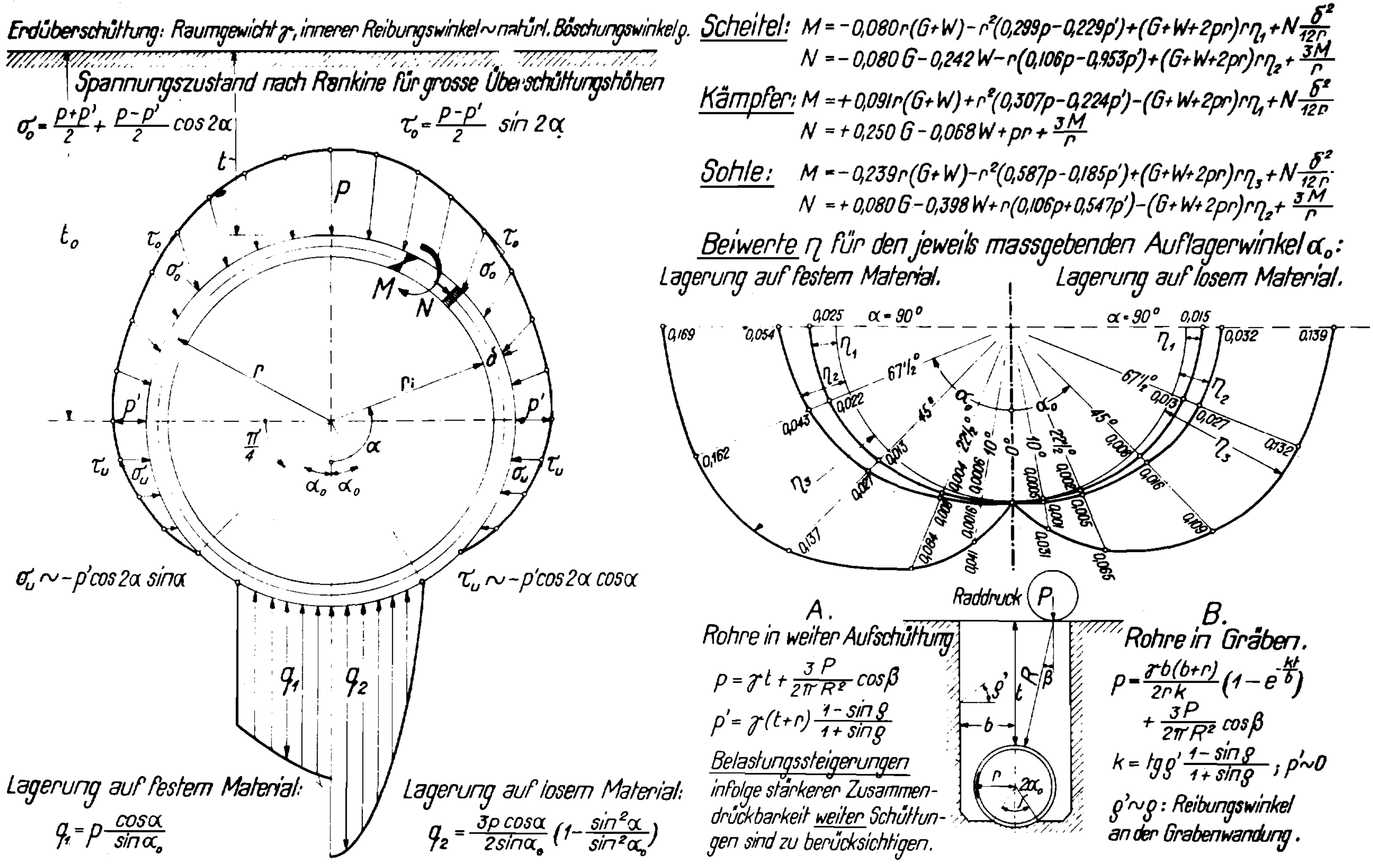

Formeln und Koeffizienten für die vereinfachte Rohrberechnung.
Innere Kräfte infolge Verteilung vertikaler Auflagerreaktionen, in Abhängigkeit vom Auflagerwinkel α_0
p ist für starre Rohre noch um den Zusatzdruck Δq (Fig. 68), infolge Zusammendrückbarkeit der Schüttung zu vergrößern

FIG. 6

Figs. 7 and 8

Section S: Ordinates positive outwards

Influence lines for the elastic bedding on the radially loaded pipe. Charactertistic of the deformability

Section S: Ordinates positive outwards

Generally valid influence lines for the inner forces on the radially loaded pipe.

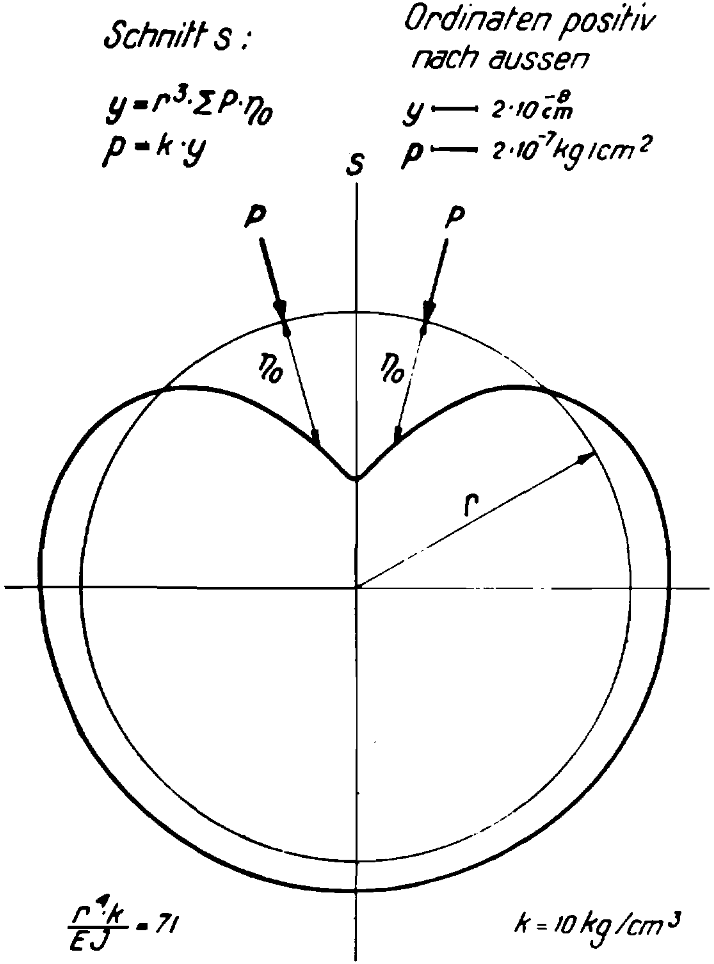

Einflußlinie für die elastische Bettung am radial belasteten Rohr· Charakteristik der Verformbarkeit:

Fig. 7

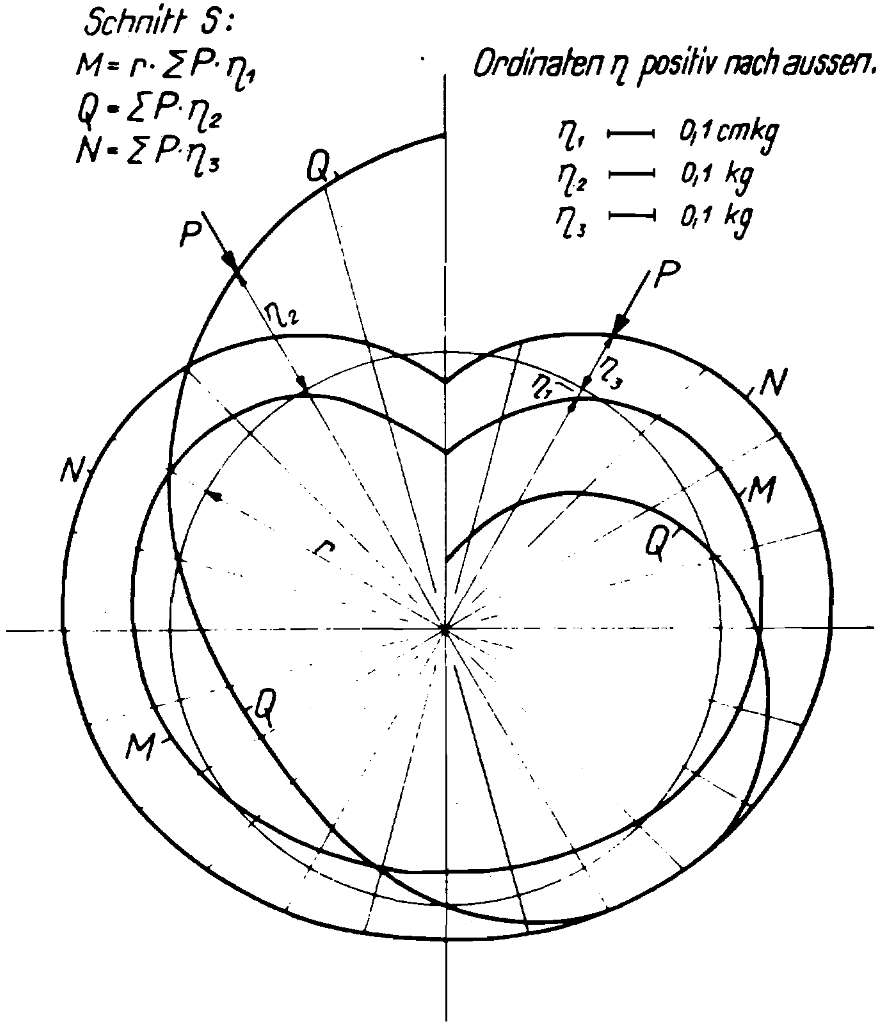

Allgemein gültige Einflußlinien für die inneren Kräfte am radial belasteten Rohr

Fig. 8

Fig. 9

Filling Material

Over filling t_o = 6 m.

Deflection line of the pipe wall
exclusion of vertical translation

Rigid Pipe

Support positive outwards.
Elastic pipe.

EARTH LOADING AND STRESSING OF AN IRON PIPE OF 66 cm. DIAMETER UNDER AN OVER FILLING OF 6 METERS.

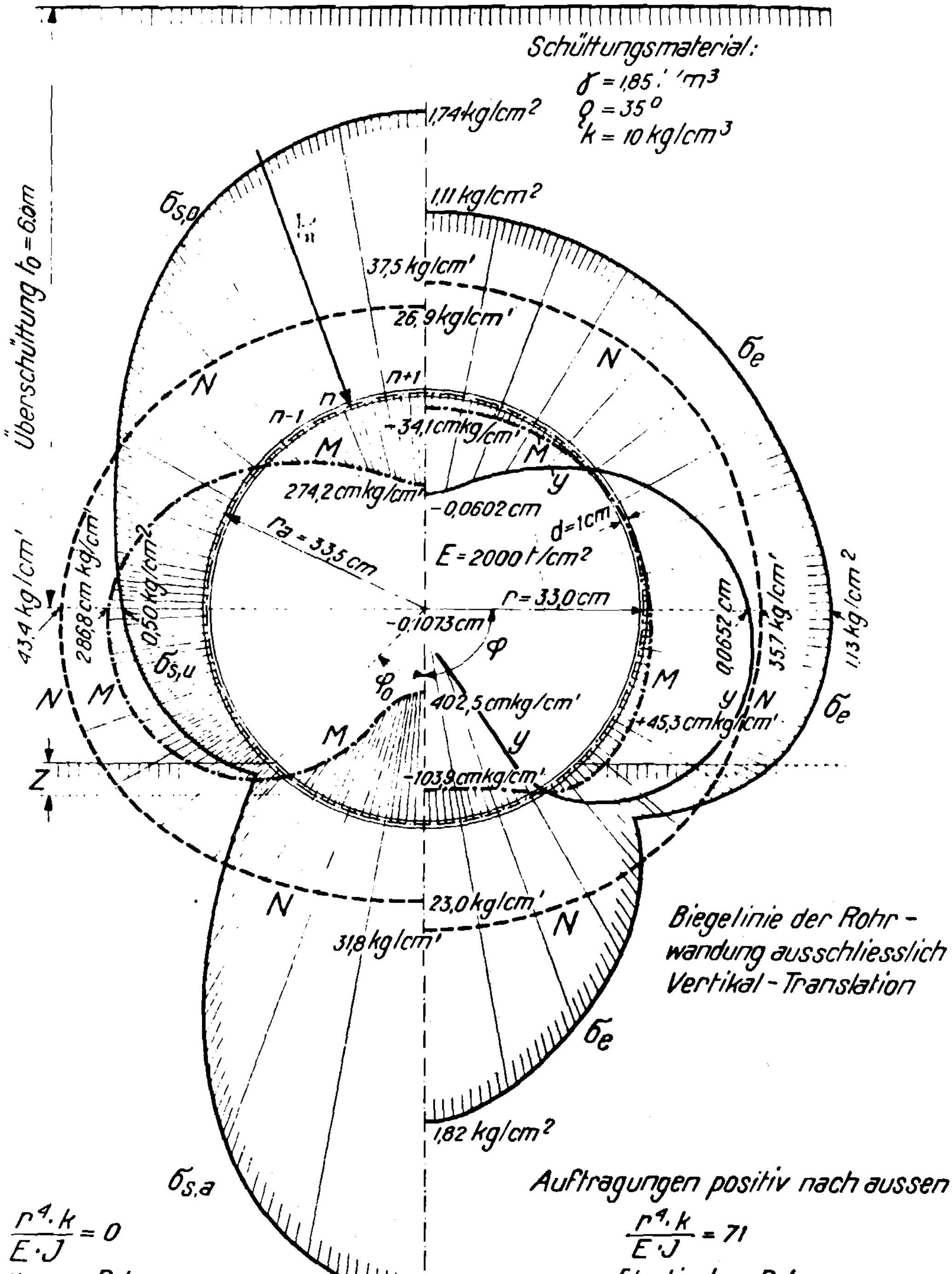

Erdbelastung und -Beanspruchung eines Eisen-Rohres von 66 cm Durchmesser unter einer Überschüttung von 6 m

Fig. 9.

Fig. 10

Inner friction angle = 35°

Specific Weight = 1.85 t/m^3

Middle line of trench depth t_o = 4.0 m.

Concrete Sole

EARTH LOADING OF A CEMENT PIPE-TRENCH CONDUIT AT 4 METERS DEPTH

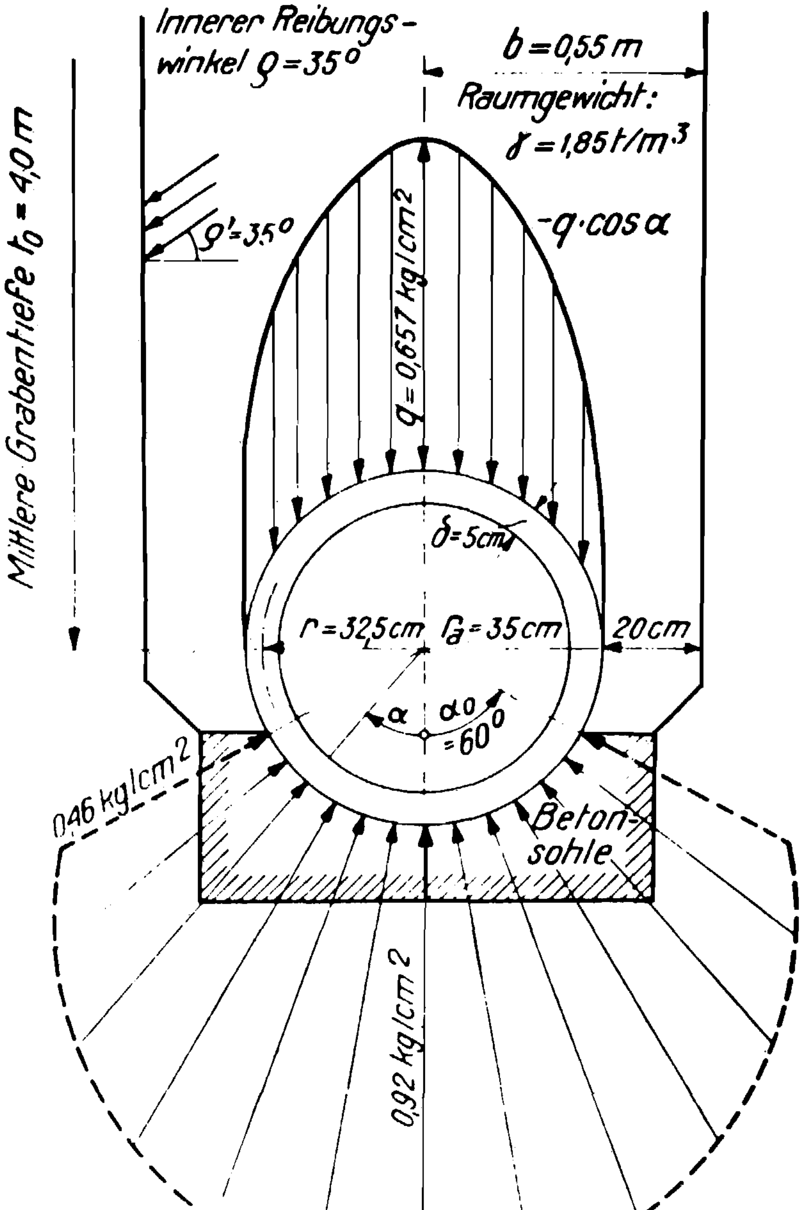

Erdbelastung einer Zementrohr-Grabenleitung in 4 m Tiefe

Fig. 10